AUTOMATYKA • 2010 • Tom 14 • Zeszyt 3/1

Anna Fabijańska*, Krzysztof Strzecha*, Tomasz Koszmider*, Marcin Bąkała*

Refining Edges to Sub-Pixel Level in Images of Molten Metals and Alloys

1. Introduction

One of the crucial problems in machine vision is edge detection in digital images [1, 2]. Edges define location and geometrical features of the objects of interest. Therefore, quality of edge detection (which is performed during low level processing) conditions accuracy of image analysis performed in the following steps of the processing.

Variety of methods for edge detection has already been proposed [3–6]. However they can be grouped into two main categories: (i) search based methods [7] and (ii) zero-crossing based methods [8].

Search based methods look for extremes in the gradient (first derivative) of an image. Most commonly, they utilize local directional maxima of the gradient magnitude which correspond with abrupt changes in image intensity. Gradient of the image is approximated by convolving input image with directional gradient masks. Popular methods belonging to this group were proposed by Sobel, Prewitt, Roberts, and Canny [1, 2, 7].

Zero crossing based methods search for zero crossings in the second derivative of the image in order to determine the edges. The second derivative is approximated using discrete Laplace filter. Because the filter is very sensitive to noise the input image is often smoothed by Gaussian filter before edge detection [1, 2, 8].

Although their popularity, well traditional, established methods for edge detection are often insufficient for practical applications in the measurement vision systems. The accuracy of edge-detectors is limited by the discrete structure of a digital raster. Moreover, the detected edge is approximate and ambiguous as different methods often produce different results for one image. It causes problems, especially when object dimensions are measured [9]. Therefore recently sub-pixel approaches are under the development.

Sub-pixel techniques are rarely used in traditional image processing. However, they are often applied in the specialized applications in photogrammetry, georeferencing and remote sensing for high-precision edge detection. Known sub-pixel approaches to edge

* Computer Engineering Department, Technical University of Lodz, Poland

detection can be qualified into two main groups: the moment-based approaches and the reconstructive approaches.

Moment – based approaches to sub-pixel edge detection express image moments by means of edge parameters. Obtained relationships are next solved in order to determine edge position with sub-pixel accuracy [10–14].

The reconstructive methods use various interpolation and curve fitting techniques in order to build continuous image functions based on discrete intensity sample values assigned to consecutive pixels. The sub-pixel location of an edge is next determined by the relevant property of the continuous image function [15–20].

This paper considers problem of refining edges in images of heat-emitting specimens of molten metals and alloys using reconstructive approach to sub-pixel edge detection. Because specimen geometrical parameters are related into surface parameters the accuracy of edge determination is crucial for the measurement process. In the considered images edges are significantly blurred due to the thermal effects. The method for improving quality of edge detection is introduced. The proposed approach determines edges with sub-pixel accuracy and eliminates weaknesses of the traditional methods for edge detection. The influence of the proposed approach on the determined values of surface tension validates its quality.

2. Definition of the problem

The aim of the research described in this paper is to determine the exact position of the border between the background and the specimen in images of heat-emitting objects. The exemplary images used in this paper are presented in Figure 1. They were obtained from computerized system for high temperature measurements of surface properties [21] and present specimen of gold at 1079 ^{o}C. The images were obtained using infrared filters of different strength. Specifically, image presented in Figure 1b was obtained using stronger filter than the one used when acquiring image from Figure 1a.

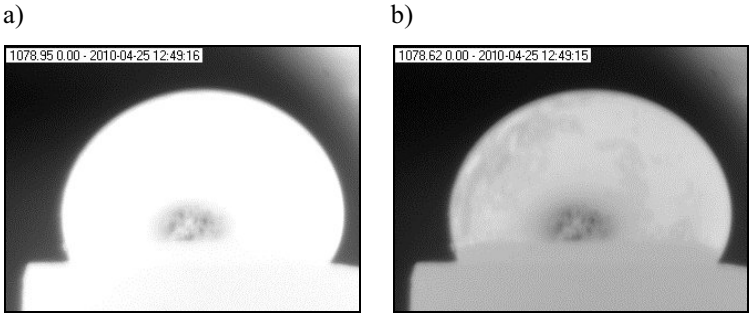

Fig. 1. Exemplary images of gold at 1079 ^{o}C: a) image obtained with filter NG4 2.5 mm; b) image obtained with filter NG4 5 mm

The considered images present bright objects on the contrasting background. However, the edges are not well defined. It's because they are significantly blurred by an "aura" i.e. glow which forms itself around the specimens due to their intense thermal radiation. An "aura" effect can be diminished by infrared filters but it can not be eliminated.

The edge between the object and the background is supposed to be located inside an "aura". However, its exact position is not clearly defined. Well established (derivative-based) methods for edge detection produce different results when applied to the same image. This effect is presented in Figure 2 which shows edges detected in image from Figure 1b using popular methods for edge detection. Most commonly, an "aura" is joined with object what increases object dimensions. This in turn influences determined values of surface tension which is calculated based on characteristic dimensions of the specimen [22].

In order to increase the accuracy of edge detection the mathematical methods, described in this paper, were applied. Approximating image derivative properties allow to refine edges detected by popular approaches to sub-pixel level. The detailed description of the proposed method is given in the following section.

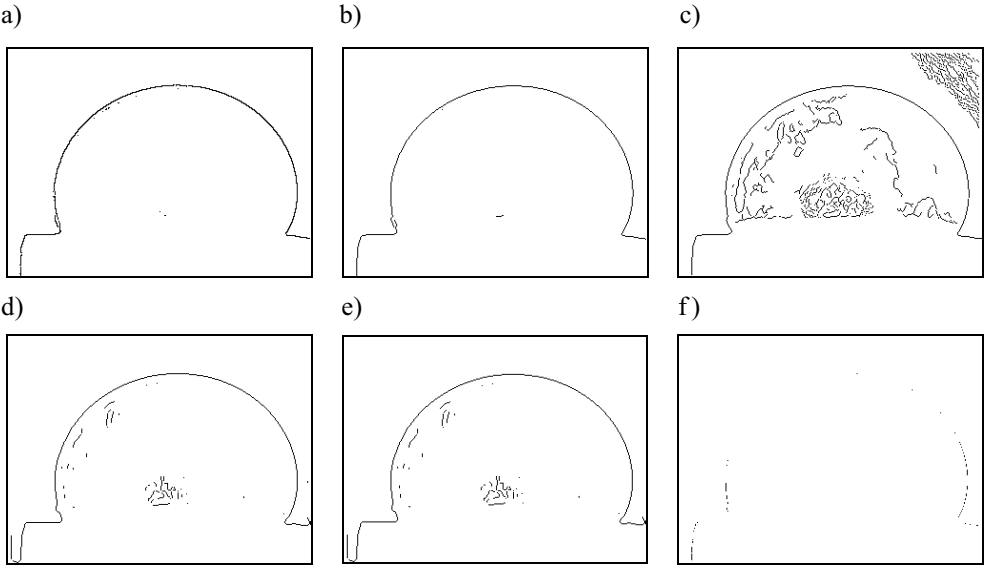

Fig. 2. Results of edge detection in exemplary image from Figure 1b obtained by the traditional approaches: a) Roberts masks; b) Sobel masks; c) Canny edge detector; d) Laplace masks; e) operator LoG; f) pixels qualified to the edge by all tested methods

3. The proposed approach

The main concept of the proposed method is to create continuous functions out of the image derivative values provided by the popular approaches to edge detection. Specifically,

Sobel gradient method and LoG edge detector are considered. The neighborhood of each coarse edge-pixel provided by these methods is examined in order to build continuous image derivatives in a given direction. When image first derivative (gradient) is considered edge position is indicated by maximum of the created (i.e. continuous) function. In case of the second image derivative, zero-crossing of the continuous function determines the edge position. This concept is explained in Figure 3.

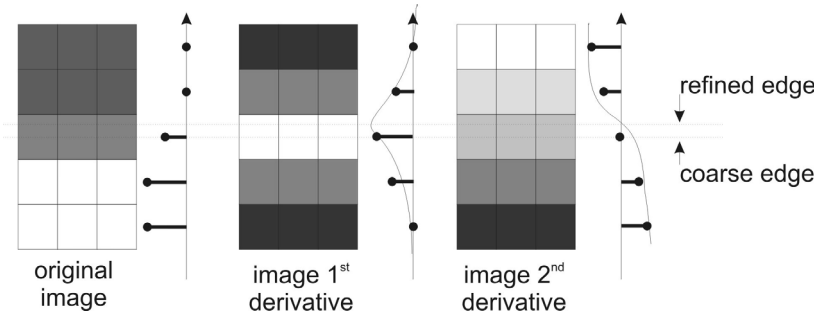

Fig. 3. Refining edges to sub-pixel level using the proposed approach

The proposed method allows to overcome limitations imposed by a discrete structure of a digital raster. It determines edge position "inside" pixel with the accuracy of tenths or even hundredths of a pixel.

Both the interpolation and the approximation can be applied for creating continuous functions out of the image derivative values. An interpolation determines function which accurately fits all image derivative values. An approximation search for function which is the closest to the given data points but not necessarily fits all of them. Their influence on properties of the refined edge is discussed in the following section.

4. Results

In this section results of applying the proposed approach to edge detection (see Sec. 3) to exemplary image from Figure 1b are presented. Specifically, Subsection 4.1 refers to results obtained using an interpolation for creating continuous functions out of the image derivative values. In Subsection 4.2 results obtained using approximation are presented. These methods were applied to refine edges provided by both the search based and the zero crossing based edge detectors. As a representative of the first group of edge detectors, Sobel gradient operator was used. The second group of edge detectors was represented by LoG operator.

4.1. Refining edges using interpolation

The following interpolation techniques provided by MATLAB environment [23] were regarded:

– nearest neighbor interpolation (referred as *nearest*);
– linear interpolation (referred as *linear*);
– piecewise cubic spline interpolation (referred as *spline*);
– piecewise cubic Hermite interpolation (referred as by *cubic*).

Figures 4 and 5 show image derivatives in the horizontal neighborhood of the most left pixel of the gold specimen from Figure 1b compared to interpolating functions build using techniques listed above. Specifically, Figure 4 refers to image first derivative obtained using Sobel gradient masks and Figure 5 refers to image second derivative obtained using LoG operator. On the horizontal axis x-coordinate of the pixel is given. The interpolating functions were obtained with the accuracy of 0.01 of pixel. The new position of the most left edge point determined (with sub-pixel accuracy) based on the interpolating functions is given in Table 1.

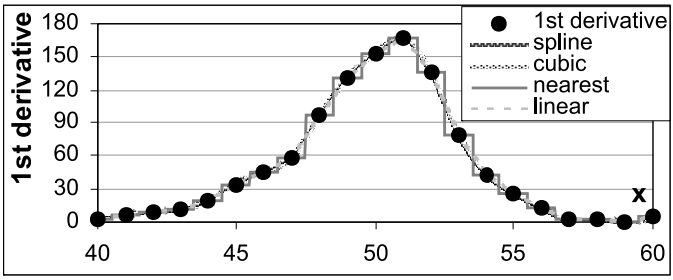

Fig. 4. Image first derivative in the horizontal neighborhood of the most left pixel of the specimen shown in Figure 1b compared to interpolating functions

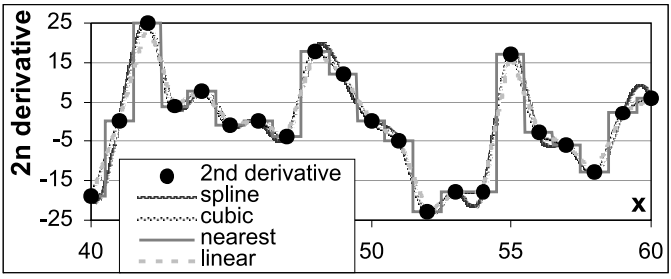

Fig. 5. Image second derivative in the horizontal neighborhood of the most left pixel of the specimen shown in Figure 1b compared to interpolating functions

Results presented in Figures 4–5 and in Table 1 show that interpolation is insufficient for refining edges using the proposed approach. Results obtained from analysis of the interpolated functions are identical with those provided by traditional (i.e. Sobel and LoG) edge

detectors. The difference between edge detected by image first and second derivative based method is not reduced. This is valid for all points of the coarse edge. Significantly better results are obtained when approximation is used. More details are given in the following subsection.

Table 1
The new position of the most left edge point determined based on interpolating functions.

Interpolating technique	Image 1st derivative	Image 2nd derivative
None	(51.0, 87.0)	(50.0, 87.0)
Nearest	(51.0, 87.0)	(50.0, 87.0)
Linear	(51.0, 87.0)	(50.0, 87.0)
Cubic	(51.0, 87.0)	(50.0, 87.0)
Spline	(50.91, 87.0)	(50.0, 87.0)

4.2. Refining edges using approximation

In the described work least-square approximation was used. The method approximates derivative function by polynomials. As previously, the technique provided by MATLAB environment was used [24].

In order to model image first derivative (gradient) second order polynomial was used. Extensive experiments have proven that in this case the trinomial square ensures the least approximation error. Gradient in the neighborhood of the most left pixel of the specimen from Figure 1b and approximating polynomial are shown in Figure 6a.

Image second derivative is approximated by linear function. Simulations have proven that in this case approximation error is the least. Image second derivative in the horizontal neighborhood of the most left pixel of the specimen from Figure 1b and approximating function are shown in Figure 6b.

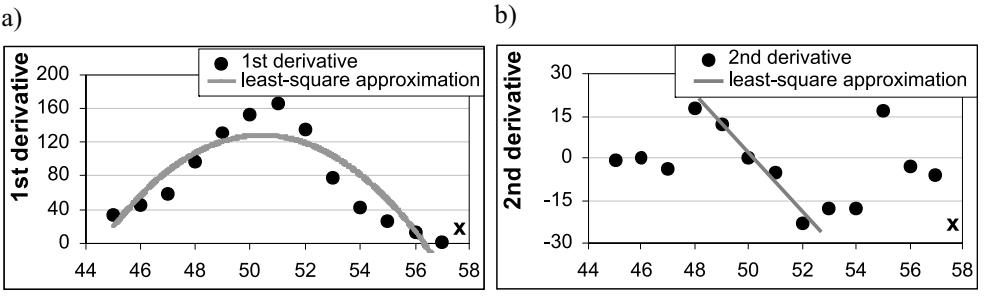

Fig. 6. Image derivative functions in the neighborhood of the most left pixel of the specimen shown in Figure 1b compared to approximating functions: a) 1st derivative; b) 2nd derivative. On the horizontal axis x-coordinate of the pixel is given

The new position of the most left edge point determined with accuracy of 0.01 pixels based on the approximating functions is given in Table 2.

Table 2
The new position of the most left edge point determined based on approximating functions

Approximating technique	Image 1st derivative	Image 2nd derivative
None	(51.0, 87.0)	(50.0, 87.0)
least-square	(50.41, 87.0)	(50.24, 87.0)

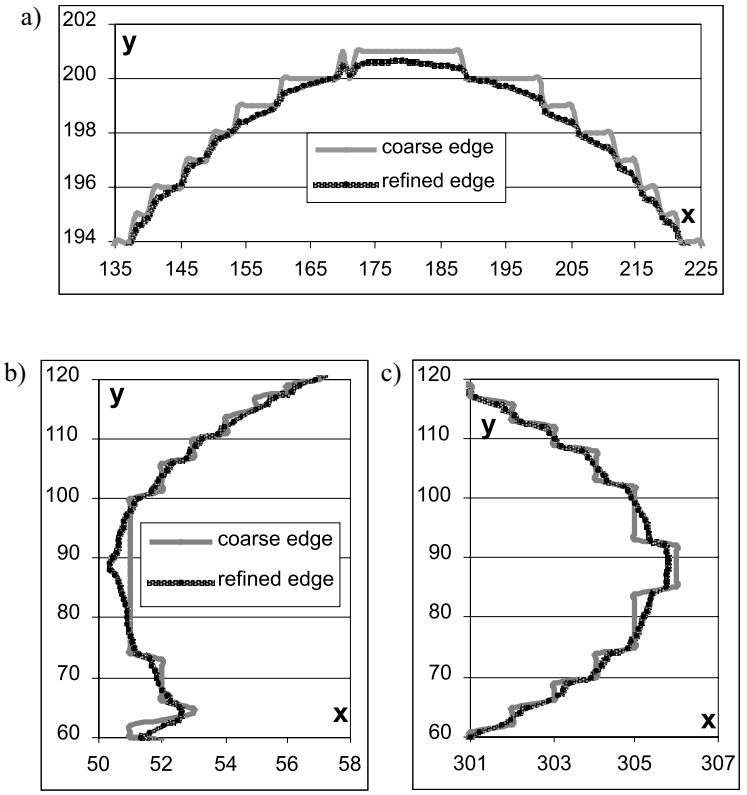

Fig. 7. Results of refining edges provided by Sobel (gradient) edge detector: a) the neighborhood of the top most pixel of the specimen profile; b) the neighborhood of the left most pixel of the specimen profile; c) the neighborhood of the right most pixel of the specimen profile

Results of refining edges using approximation in the exemplary image from Figure 1b are shown in Figures 7 and 8. Edges refined to sub-pixel level are compared with those provided by the considered traditional approaches. Specifically, in Figure 7 results of

re-fining edges provided by Sobel gradient detector are shown. Figure 8 presents results of refining edges provided by LoG operator. In order to increase the readability of the results only the most important details of the specimen shape are presented. Specifically, edges in the neighborhood of the top most, left most and right most pixel of the specimen are regarded. Position of these points influences determined values of surface tension. In order to obtain edges presented in Figures 7a and 8a gradient sample values in vertical direction were considered. Edges from Figures 7bc and 8bc resulted from gradient approximation in horizontal direction.

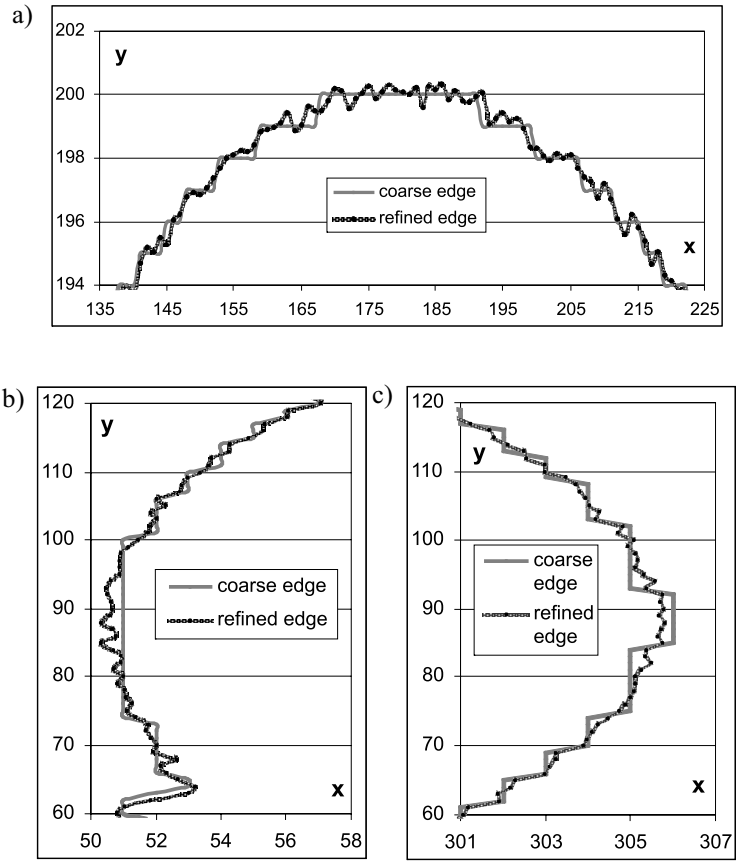

Fig. 8. Results of refining edges provided by LoG operator: a) the neighborhood of the top most pixel of the specimen profile; b) the neighborhood of the left most pixel of the specimen profile; c) the neighborhood of the right most pixel of the specimen profile.

Results presented in Figures 7–8 and Table 2 clearly show that approximation improves edge properties. The refined edges are smoother and significantly more regular than they were before. The improvement of edge smoothness is particularly noticeable when

the edge obtained using Sobel method is refined. The edges refined after application the LoG operator are more irregular but they are significantly better than the edges produced by the traditional approaches.

In both cases (i.e. in case of method based on image first and second derivative), the edges are significantly more consistent with the specimen shape after refining.

Presented results clearly show, that refining edges influences coordinates of the edge points. Specifically, the top most, the left most and the right most are slightly moved. This in turn influences determined values of surface tension. It should be also underlined that the discrepancy between edges provided by first and second derivative based edge detector is diminished due to refining.

5. Validation

The quality of the proposed method was assessed by means of the specimen characteristic dimensions (see Fig. 9) and values of surface tension determined using Equation (1).

$$\gamma = g \cdot \Delta\rho \cdot \alpha^2 \tag{1}$$

where:

γ – surface tension,
g – gravity acceleration,
$\Delta\rho$ – gradient of densities,
α^2 – parameter determined using (2).

$$\left(\frac{2\alpha}{d^2}\right)^2 = \left(\frac{2h}{d}\right)^2 - 0.660\left(\frac{2h}{d}\right)^3\left[1 - 4.05\left(\frac{2h}{d}\right)^2\right] \tag{2}$$

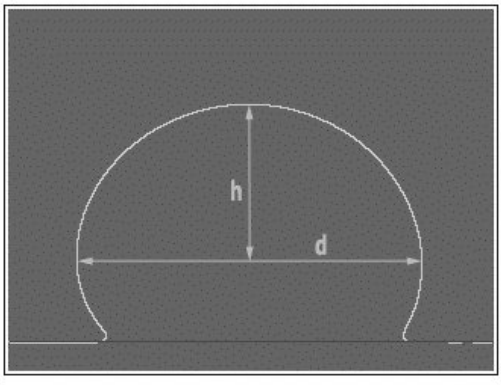

Fig. 9. Drop characteristic dimensions: d – maximum width, h – maximum height

The obtained results of surface tension measurements, based on the refined edges, were compared with the numerical data presented in the literature. For refining of edges approximation was used. The presented comparison is only tentative as there is no "gold standard" for surface tension of metals. The high-temperature measurements of surface tension are related to different problems arising from the activity of liquid metals and sensitivity of surface phenomena to impurities, temperature, pressure and atmosphere. Therefore, recent results vary, depending on the method used for the measurements [25].

In Table 3 comparison of drop characteristic dimensions d and h (see Fig. 9) calculated for exemplary specimen from Figure 1b with the pixel and the sub-pixel accuracy is presented. Header "*1st derivative*" corresponds with Sobel edge detector and "*2nd derivative*" corresponds with LoG operator. Specimen characteristic dimensions (in pixels) are given in the first two rows. The last row presents values of surface tension calculated on the basis of characteristic dimensions d and h. It should be underlined, that before calculation of surface tension dimensions d and h should be multiplied by the pixel dimensions.

The comparison shown in Table 3 proves that refining edges using approximation improves quality of edge detection. The improvement manifests itself in smaller difference between edges produced by using the image first and second derivatives. The disparity in specimen dimensions approximated after applying Sobel and LoG with pixel accuracy is remarkably diminished.

Table 3
Comparison of drop characteristic dimensions and the determined values of surface tension

	1st derivative		2nd derivative	
	Pixel accuracy	Sub-pixel accuracy	Pixel accuracy	Sub-pixel accuracy
d [pixels]	256	255.48	255	255.48
h [pixels]	114	111.75	113	112.33
Surface tension [mN/m]	1227.59	1180.67	2935.91	1192.61

According to the recent results [14], surface tension of gold at 1079 ^{o}C equals 1148 mN/m. Compared to this value, the results of a surface tension obtained using the sub-pixel approach are more accurate than the results obtained before approximation based refining. The improvement in accuracy of surface tension determination is apparent especially in case of edges determined by LoG operator.

6. Conclusions

In this paper problem of precise edge detection in images of heat-emitting objects was considered. The approach for refining edges to sub-pixel level was introduced. The pro-

posed approach creates continuous functions out of the image derivative values provided by the other known methods for edge detection. Characteristic points of the continuous functions (i.e. maxima or zero-crossings) determine edge position with sub-pixel level.

The influence of the technique used for creating continuous functions on the properties of the refined edge was regarded. Interpolation and approximation methods were applied to make image first and second derivative continuous. The simulation results proved that the best results are obtained when image first derivative is approximated using the trinomial square. The refined edge is most regular and accurately fits the specimen shape when the second order polynomial is used. The visual impression is proven by the determined values of surface tension.

Although the proposed method was developed for a certain class of images it can be successfully applied in a wide spectrum of applications.

Acknowledgements

The presented work is supported by the Ministry of Science and Higher Education of Poland from founds for science in 2010–2012 as a research project no. N N519 403037.

References

[1] Gonzalez R.C., Woods R.E., *Digital Image Processing*. Prentice Hall, Upper Saddle River, New Jersey, 2001.

[2] Young T., Gerbrands J.J., van Vliet L.J., *Fundamentals of Image Processing*. The Netherlands at the Delft University of Technology, 1998.

[3] Senthilkumaran N., Rajesh R., *Edge Detection Techniques for Image Segmentation – A Survey of Soft Computing Approaches*. International Journal of Recent Trends in Engineering, vol. 1, 2009, 250–254.

[4] Basu M., *Gaussian-Based Edge-Detection Methods – A Survey*. IEEE Transactions on Systems, Man, and Cybernetics, Part C: Applications and Reviews, vol. 32, No. 3, 2002, 252–260.

[5] Ziou D., Tabbone S., *Edge Detection Techniques – An Overview*. International Journal of Pattern Recognition and Image Analysis, vol. 8, 1998, 537–559.

[6] Davis L.S., *A Survey of Edge Detection Techniques*. Computer Graphics and Image Processing, vol. 4, 1975, 248–270.

[7] Marr D., Hildreth E., *Theory of Edge Detection*. Proc. of Royal Society, vol. B-207, 1980, 187–217.

[8] Haralick R.M., *Zero Crossing o Second Directional Derivative Edge Operator*. SPIE Symposium on Robot Vision, vol. 336, Washington, USA, 1982, 91–99.

[9] Fabijańska A., Koszmider T., Strzecha K., Bąkała M., *Precise Edge Detection in Images of Melted Specimens of Metals and Alloys*. Proc. IEEE Int. Conf. Perspective Technologies and Methods in Mems Design, Lviv-Polyana, Ukraine, 2010, 67–70.

[10] Machuca R., Gilbert A.L., *Finding Edges in Noisy Scenes*. IEEE Transactions on Pattern Analysis and Machine Intelligence, vol. PAMI-3, 1981, 103–111.

[11] Tabatabai A.J., Mitchell O.R., *Edge Location to Sub Pixel Values in Digital Imagery*. IEEE Transactions on Pattern Analysis and Machine Intelligence, vol. 6, No. 2, 1984, 188–20l.

[12] Lyvers E.P., Mitchell O.R., Akey M.L., Reeves A.P., *Subpixel Mesurements Using a Moment-Based-Edge Operator*. IEEE Transactions on Pattern Analysis and Machine Intelligence, vol. 11, No. 12, 1989, 1293–1309.
[13] Ghosal S., Mehrotra R., *Orthogonal Moment Operators for Subpixel Edge Detection*. Pattern Recognition Letters, vol. 26, No. 2, 1993, 295–305.
[14] Bin T.J., Lei A., Jiwen C., Wenjing K., Dandan L., S*ubpixel Edge Location Based on Orthogonal Fourier-Mellin Moments*. Image and Vision Computing, vol. 26, No. 4, 2008, 563–569.
[15] Li, Y.-S., Young, T.Y., Magerl J.A., *Subpixel Edge Detection And Estimation With a Microprocessor-Controlled Line Scan Camera*. IEEE Transactions on Industrial Electronics, vol. 35, No. 1, 1988, 105–112.
[16] Eugenio F., Marques F., Marcello J., *Pixel and Sub-Pixel Accuracy in Satellite Image Georeferencing Using an Automatic Contour Matching Approach*. Proc. Int. Conf. Processing, vol. 1, 2001, 822–825.
[17] Bailey D.G., *Sub-pixel Profiling*. Proc. 5th Int. Conf. Information, Communications and Signal Processing, 2005, 1311–1315.
[18] Breder R., Estrela V.V., de Assis J.T., *Sub-Pixel Accuracy Edge Fitting By Means of B-Spline*. IEEE Int. Workshop on Multimedia Signal Processing, 2009, 1–5.
[19] Min W., Xiangjin Z., Xinhan H., *A Novel Sub-Pixel Edge Detection for Micro-Parts Manipulation*. Proc. IEEE Int. Conf. Robotics and Biomimetics, 2009, 1297–1301.
[20] Li C., Xu G., *Sub-pixel Edge Detection Based on Polynomial Fitting for Line-matrix CCD Image*. Proc. 2nd Int. Conf. Information and Computing Science, 2009, 262–264.
[21] Fabijańska A., Sankowski D., *Computer Vision System for High Temperature Measurements of Surface Properties*. Machine Vision and Applications, Springer, vol. 20, DOI: 10.1007/s00138-008-0135-1, 2009, 411–421.
[22] Strzecha K., Koszmider T., *Drop Shape Analysis for Measurements of Surface Tension and Wetting Angle of Metals at High Temperatures*. Proc. IEEE Int. Conf. Perspective Technologies and Methods in Mems Design, Lviv-Polyana, Ukraine, 2008, 57–59.
[23] MATLAB, *Interp1* on-line documentation, http://www.mathworks.com/access/. helpdesk/help/techdoc/ref/interp1.html, accessed May 2010.
[24] MATLAB, *polyfit* on-line documentation, http://www.mathworks.com/access/ helpdesk/help/techdoc/ref/polyfit.html, accessed May 2010.
[25] Mills K.C., Su Y.C., *Review of Surface Tension Data for Metallic Elements and Alloys: Part 1 – Pure Metals*. International Materials Reviews, vol. 51, Maney Publishing, 2006, 329–351.